



Modeling COVID-19 dynamics in the sixteen West African countries



Sewanou H. Honfo, Hemaho B. Taboe, Romain Glèlè Kakai*

Laboratoire de Biomathématiques et d'Estimations Forestières, Faculty of Agronomic Sciences, University of Abomey-Calavi, Calavi, Bénin

ARTICLE INFO

Article history:

Received 19 September 2020

Revised 27 November 2021

Accepted 20 October 2022

Editor DR B Gyampoh

Keywords:

SARS-CoV-2

Detection rate

Peak time and size

Final epidemic size

Attack ratio

Africa

ABSTRACT

The COVID-19 pandemic is currently causing several damages to the world, especially in the public health sector. Due to identifiability problems in parameters' estimation of complex compartmental models, this study considered a simple deterministic susceptible-infectious-recovered (SIR)-type model to characterize the first wave and predict the future course of the pandemic in the West African countries. We estimated some specific characteristics of the disease's dynamics, such as its initial conditions, reproduction numbers, true peak and peak of the reported cases, with their corresponding times, final epidemic size and time-varying attack ratio. Our findings revealed a relatively low proportion of susceptible individuals in the region and the different countries (1.2% across West Africa). The detection rate of the disease was also relatively low (0.9% for West Africa as a whole) and < 2% for most countries, except for Gambia (12.5 %), Cape-Verde (9.5%), Mauritania (5.9%) and Ghana (4.4%). The reproduction number varied between 1.15 (Burkina-Faso) and 4.45 (Niger), and most countries' peak time of the first wave of the pandemic was between June and July. Generally, the peak time of the reported cases came a week (7-8 days) after the true peak time. The model predicted for the first wave, 222,100 actual active cases in the region at the peak time, while the final epidemic size accounted for 0.6% of the West African population (2,526,700 individuals). The results showed that COVID-19 has not severely affected West Africa as in other regions. However, current control measures and standard operating procedures should be maintained over time to accelerate a decline in the observed trends of the pandemic.

© 2022 The Author(s). Published by Elsevier B.V. on behalf of African Institute of Mathematical Sciences / Next Einstein Initiative.

This is an open access article under the CC BY-NC-ND license (<http://creativecommons.org/licenses/by-nc-nd/4.0/>)

Introduction

COVID-19 is a severe acute respiratory syndrome caused by the new coronavirus, SARS-CoV-2, which emerged from Wuhan, Hubei Province (China) towards the end of 2019 [1,2]. It is currently the most important threat to global public health. By August 15th, 2020, about 21,026,758 total confirmed cases and 755,786 deaths were recorded worldwide [3]. The disease has rapidly spread around the world (about 212 countries) [4], including the 54 African countries. By mid-August 2020, The World Health Organisation (WHO) reported 936,062 and 152,483 confirmed cases and 18,286 and 2,351 deaths

* Corresponding author.

E-mail address: romain.glelekakai@fsa.uac.bj (R. Glèlè Kakai).

across Africa and the West-African region, respectively [3]. Healthcare services in the region have particularly faced critical times, making sensitive decisions regarding patients and their treatment [5]. It is clear that the COVID-19 pandemic has severely affected people's life, health and economy. Actually, it led to a significant increase in the demand for hospital beds and artificial respirators (mechanic and non-invasive). According to the WHO global health observatory data, most countries in West Africa have less than five hospital beds and two medical doctors per 10,000 of the population, while 50% of the countries have health expenditures lower than US\$50 per capita [6]. In contrast, European countries such as Italy and Spain have 34 and 35 hospital beds with 41 medical doctors per 10,000 of the population, and US\$2,840 and US\$2,506 per capita expenditure, respectively [7]. Moreover, medical staff worldwide have been directly exposed to infections [8]. Since vaccines are still under development, and antiviral drugs are not available for effective curative treatment of COVID-19 infections, the actual cure practice is hospitalization and intensive care unit management [9]. Prevention measures used are essentially non-pharmaceutical interventions such as regular hand washing with soap, mask-wearing and social distancing. To be efficient, these non-pharmaceutical measures require a good understanding of the dynamic of the spread of the disease to aid in the decision-making of their use.

Mathematical and statistical models can be useful tools for decision-making in public health. They are also important in ensuring the optimal use of resources to reduce the morbidity and mortality associated with epidemics through estimation and prediction [10]. The prediction of essential epidemiological parameters, such as the peak time, the duration and the final size of the outbreak, is crucial for policymakers and the public health authorities to make appropriate decisions for the control of the pandemic [9]. Therefore, modelling and forecasting the numbers of confirmed and recovered COVID-19 cases could play an important role in designing better strategies to control the spread of COVID-19 in the world [4]. Since the appearance of the first COVID-19 case in the world, several studies have been conducted to model the dynamics of the disease. The main methods used were: deterministic modelling techniques [11–13], autoregressive time series models based on two-piece scale mixture normal distributions [4], stochastic modelling methods [14,15], machine learning techniques [16,17], growth models [18,19] and bayesian method [17].

Among these modeling techniques, deterministic models are the most considered because of their simplicity. However, they fail to provide accurate results due to the non-identifiability problems when the number of compartments and the number of parameters are high [2]. Actually, complex deterministic models have proven to be less reliable than simpler models such as the SIR model framework [2], which performs better in describing trends in epidemiological data. This under-performance may be worse when meta-population confirmed-cases data are considered. However, only a few studies related to COVID-19 in Africa used mathematical models and prevalence data to study the dynamics, and analyze the causes and key factors of the outbreak [1,11,20]. A recent study [11] assessed the current pattern of COVID-19 spread in West Africa using a deterministic compartmental SEIR-type model.

In this study, we used a simple deterministic susceptible–infectious–recovered (SIR)-type model to characterize the first wave of the pandemic and predict its future trends in West Africa. Specifically, we aimed to estimate some specific characteristics of COVID-19 dynamics (initial conditions of the pandemic, reproduction numbers, true peak, reported peak and their times and dates, final epidemic size and time-varying attack ratio). The originality of this work is that it focused on the 16 West African countries and the whole region as well. It is the first study dealing with the dynamics of the pandemic in each of the West African countries. Moreover, this study used a novel approach to estimate the parameters of compartmental models, based on a cross-validation procedure for estimations. This approach alleviates the problem of non-identifiability of parameters and ensures accurate estimates [21].

Methods

Model description

Problems of identifiability in parameters' estimation in deterministic compartment models (especially complex models) are common in epidemiological modelling studies, which often imply biased estimations of parameters. In these situations, simpler models, which over-perform complex models in estimating reliable parameters, are recommended [2]. Hence, in this study, the SIR model [22] was considered with two removal rates as illustrated in the system below [23]:

$$\begin{cases} \frac{dS}{dt} = -\frac{\beta SI}{N}, \\ \frac{dI}{dt} = \frac{\beta SI}{N} - (v_1 + v_2)I, \\ \frac{dR}{dt} = (v_1 + v_2)I. \end{cases} \quad (1)$$

with $N = S + I + R$, $S(0) = S_0 > 0$, $I(0) = I_0 > 0$, $R(0) = R_0 \geq 0$ and $N(0) = N = S_0 + I_0 + R_0$.

In Eq. (1), $S = S(t)$, $I = I(t)$ and $R = R(t)$, representing the number of susceptible, infected and removed individuals at time t , respectively; while N is defined as the total population size for the disease transmission. The parameters β , v_1 and v_2 are the transmission rate, the removal rate of reported infected individuals (detected) and the removal rate of infected individuals due to all other unreported causes (mortality, recovery or other reasons), respectively. We considered the removal rate v_2 as constant with value $v_2 = 1/10$ [24]. From the second differential equation of Eq. (1), it could be noticed that $v_1 I_0$

represents the daily confirmed cases (I_{r0}) at time 0 of the outbreak. Thus, the relationship between the initial number of infected individuals and the detection rate, v_1 , is $I_0 = I_{r0}/v_1$, was used in the estimation process.

Data consideration and parameter estimation procedure

For each country, the data considered for the modelling spans the period from the date of detection of the first case of COVID-19 in the country and August 12, 2020. Data considered were the daily numbers of reported cases that were assimilated to $v_1 I$. These data were downloaded from the Global Rise of Education website [25]. Table A1 presents the demographic patterns [26], initial dates of the pandemic [25] and testing efforts (identification of new cases) of the countries [26]. We fitted the model Eq. (1) to the observed daily cases to study the dynamics of the COVID-19 pandemic in the 16 West African countries.

To improve the prediction power of Eq. (1), we used a cross-validation procedure of parameter estimation, where 90% of the observations were considered to estimate values of the five unknown model parameters ($S_0, I_0, R_0, \beta, v_1$) and the remaining observations were used to validate the model. The Root Mean Square Error (RMSE) statistic was used as the measure of estimation precision:

$$RMSE = \sqrt{\frac{\sum_{i=1}^k (\hat{\theta} - \theta)^2}{k}}, \quad (2)$$

where $\hat{\theta}$ and θ are the predicted and observed number of daily cases, respectively; k is the number of observations considered. $RMSE$ is used to compare the prediction errors of different models. Its values range from 0 and ∞ , with the lowest values indicating better estimation precision [27]. We considered as $RMSE_1$, the Root Mean Square Error computed on the 90% of the observations and $RMSE_2$, computed on the remaining observations (10%).

The solutions of Eq. (1) were obtained using the built-in function *ODE45* of Matlab [28]. Then, the non linear least square technique was performed to estimate the five parameters in Eq. (1) given starting values, using the built-in function *fminsearchbnd* of Matlab [28].

Afterwards, we simulated 2,000 different starting values of the five parameters using a resampling method (function *resample* of Matlab) for S_0, I_0 and R_0 and the uniform distribution (function *rand* of Matlab) for β and v_1 . Then, we estimated for each of the starting points, values of the five parameters using the non-linear least square technique described above. The final values considered for these parameters were those related to both the smallest values of $RMSE_2$ and $RMSE_1$ to guarantee a good fit of the model and a good predictive power. At the end of this process, we obtained reliable estimates of the model parameters with 95 % confidence intervals. Curves were plotted to show evolution trends of predicted daily new COVID-19, daily reported cases and the attack ratio for the 16 countries. With the estimated values of the five parameters from Eq. (1), the COVID-19 dynamic in each country was characterized by computing the following parameters with their 95% confidence intervals.

- *Reproduction number, \mathcal{R}_0* [29]: it is the average number of secondary infections, caused by an average infected individual (during his infectious period), in a fully constituted population:

$$\mathcal{R}_0 = \frac{\beta}{v_1 + v_2}. \quad (3)$$

- *Running reproductive number, \mathcal{R}_e* [29]: it measures the number of secondary infections caused by a single infected individual in the population at time t :

$$\mathcal{R}_e = \frac{S(t)}{N} \frac{\beta}{v_1 + v_2}. \quad (4)$$

- *True peak size, n_{pp} , and True peak time, T_{pp}* . The true peak size indicates the largest daily number of new infectious cases in the population:

$$n_{pp} = \max\left(\beta \frac{SI}{N}\right), \quad (5)$$

while the true peak time, T_{pp} , represents the time at which the largest daily new infected cases is obtained. These two parameters were determined numerically. - *Peak size of reported cases, n_{rp} , and Peak time of reported cases, T_{rp}* . The peak size of reported cases indicates the largest number of daily confirmed cases:

$$n_{rp} = \max(v_1 I), \quad (6)$$

while the peak time of reported cases is the associated time to n_{rp} . These were determined numerically. - *Maximum number of active cases, I_{max}* : since $I_0, R_0 \ll S_0$, we assumed the number of initial susceptible individuals to be approximately equal to N ($S_0 \approx N$). Thus, I_{max} can be approximated as follow [29]:

$$I_{max} \approx N \left[1 - \frac{1}{\mathcal{R}_0} (1 + \log(\mathcal{R}_0)) \right]. \quad (7)$$

- *Final epidemic size, I_{total}* [29]: it is the total number of cases over the course of the epidemic wave.

$$I_{total} = S_0 - S_{\infty}; \quad S_{\infty} = \lim_{t \rightarrow \infty} S(t), \quad (8)$$

Table 1Estimates with 95% confidence intervals of the initial parameters of the SIR-model; $\nu_2 = 0.10$ is constant for all countries.

Country	S_0 ($\times 10^5$) [95%CI]	I_0 [95%CI]	R_0 [95%CI]	β [95%CI]	ν_1 [95%CI]	RMSE ₂
Benin	1.212 [1.211-1.214]	200 [197-203]	39 [37-40]	0.148 [0.145-0.151]	0.005 [0.004-0.006]	31.7
Burkina-Faso	2.175 [2.145-2.206]	174 [164-183]	160 [149-172]	0.121 [0.121-0.122]	0.006 [0.005-0.007]	8.0
Cape-Verde	0.517 [0.460-0.573]	21 [17-26]	97 [91-102]	0.226 [0.221-0.231]	0.095 [0.092-0.098]	98.8
Côte d'Ivoire	2.643 [1.265-4.021]	73 [23-124]	8 [6-9]	0.178 [0.175-0.181]	0.014 [0.011-0.017]	65.6
Gambia	0.24 [0.21-0.26]	8 [7-8]	0 [0-2]	0.259 [0.256-0.262]	0.125 [0.124-0.126]	15.2
Ghana	3.291 [2.388-4.193]	46 [24-68]	81 [80-83]	0.20 [0.197-0.203]	0.044 [0.041-0.047]	462.0
Guinea	3.789 [3.428-4.151]	229 [206-251]	85 [82-88]	0.146 [0.145-0.148]	0.004 [0.004-0.005]	35.7
Guinea-Bissau	3.458 [3.452-3.497]	1990 [1970-2011]	4 [2-5]	0.146 [0.144-0.147]	0.001 [0.000-0.004]	15.2
Liberia	0.507 [0.506-0.508]	100 [98-102]	87 [85-89]	0.146 [0.143-0.149]	0.010 [0.007-0.013]	153.4
Mali	2.240 [2.215-2.265]	1175 [1139-1211]	199 [194-203]	0.167 [0.165-0.169]	0.002 [0.000-0.005]	39.1
Mauritania	0.466 [0.291-0.641]	17 [8-26]	42 [41-44]	0.221 [0.216-0.225]	0.059 [0.055-0.063]	40.7
Niger	2.652 [1.578-3.276]	1203 [1250-1296]	39 [47-54]	0.448 [0.441-0.455]	0.001 [0.000-0.001]	2.1
Nigeria	20.886 [10.651-31.121]	252 [212-293]	110 [102-117]	0.173 [0.169-0.178]	0.004 [0.000-0.009]	2926.6
Senegal	1.976 [0.723-3.230]	61 [16-138]	99 [98-101]	0.161 [0.160-0.163]	0.016 [0.014-0.019]	48.4
Sierra-Leone	0.799 [0.797-0.801]	200 [191-209]	5 [3-6]	0.166 [0.160-0.171]	0.005 [0.000-0.012]	7.4
Togo	0.830 [0.662-0.999]	42 [38-45]	28 [26-29]	0.144 [0.143-0.146]	0.024 [0.022-0.026]	8.0
West Africa	48.667 [31.820-62.722]	5811 [5559-6194]	1112 [1043-1144]	0.152 [0.151-0.152]	0.009 [0.007-0.010]	1463.3

S_0 , I_0 and R_0 : initial number of Susceptible, Infected and Removed individuals, respectively ($t = 0$); ν_1 : detection rate of infected individuals; β_0 : Estimated transmission rate; $RMSE_2$: Root Mean Square Error computed on the remaining observation (cross-validation).

S_∞ can be approximated considering the entire population as initially susceptible ($S_0 \approx N$); hence, following [29]:

$$\log\left(\frac{S_\infty}{N}\right) = \mathcal{R}_0\left(\frac{S_\infty}{N} - 1\right). \quad (9)$$

For each country, the equation Eq. (9) was solved numerically to determine S_∞ through an iterative process. - *Attack ratio*, A_r [23]: it is the fraction of susceptible population that becomes infected. It is calculated along the epidemic wave as follows:

$$\begin{aligned} A_r(t) &= \frac{S_0 + I_0 + R_0 - S(t)}{S_0 + I_0 + R_0} \\ &= \frac{N - S(t)}{N}. \end{aligned} \quad (10)$$

For West Africa as a whole, S_0 , I_0 and R_0 were first computed by summing the corresponding estimated values of the 16 countries. Afterwards, the model (9) was fitted to daily reported cases of the region using initial conditions computed. This allowed the estimation of β and ν_1 and the computation of the characteristics of COVID-19 dynamics across the region.

Results

Patterns of the first wave of COVID-19 transmission in West Africa

Table A1 (Appendix A) presents demographic patterns and testing efforts in the West African region. It reveals great heterogeneity in the region in terms of population density and testing efforts. Countries such as Cape-Verde, Mauritania and Ghana have put relatively more effort into identifying infected individuals; while Niger, Nigeria and Guinea are countries with the lowest number of tests per one million people.

Combining both the testing effort and the mean number of reported cases per test indicates a relatively less testing effort to identify many infected individuals (Guinea and Gambia). On the other hand, countries like Cape-Verde, Benin and Togo had put relatively more effort into finding few COVID-19 cases (Table A1).

Results obtained from the estimation of initial conditions of the COVID-19 pandemic in West Africa revealed a relatively low proportion of susceptible individuals in most countries (about 1% of their total population). However, countries such as Guinea-Bissau and Cape-Verde showed a relatively large proportion of susceptible individuals to COVID-19 with 17.5% and 2.4% of their total populations, respectively. The proportion of the susceptible individuals across West Africa was also relatively low (1.2%) (Table A1 and Table 1). Moreover, before the detection of the first cases, infected individuals were present in the population of all the countries with some already recovered individuals. The detection rate of infected individuals was relatively low (less than 1%) for Benin, Burkina, Mali, Niger, Nigeria, Sierra-Leone and West Africa as a whole. However, some countries such as Gambia (12.5 %), Cape-Verde (9.5%), Mauritania (5.9%) and Ghana (4.4%) recorded the highest detection rates (Table 2).

In most countries, the model estimated an average of one new case of infection caused by an infected individual during the infectious period (\mathcal{R}_0), except for Sierra-Leone, Nigeria, and Côte d'Ivoire with $\mathcal{R}_0 \approx 2$ and Niger, which recorded the highest reproduction number ($\mathcal{R}_0 \approx 4$) (Table 2).

Table 2

Epidemiological statistics with their 95% confidence intervals (CI) indicating the dynamics of COVID-19 in the whole west African and per country.

Country	\mathcal{R}_0 [95%CI]	T_{rp} [95%CI]	n_{rp} [95%CI]	T_{pp} [95%CI]	n_{pp} [95%CI]	I_{max} [95%CI]($\times 10^4$)	I_{total} [95%CI]($\times 10^4$)
Benin	1.41 [1.38-1.43]	114 [112-116]	29 [24-34]	104 [103-107]	634 [558-710]	0.57 [0.53-0.61]	6.3 [6.3-6.4]
Burkina-Faso	1.15 [1.14-1.15]	239 [234-245]	12 [11-13]	229 [223-235]	218 [213-222]	0.19 [0.19-0.20]	5.4 [5.3-5.4]
Cape-Verde	1.16 [1.14-1.18]	149 [148-150]	50 [46-53]	144 [143-145]	103 [89-117]	0.05 [0.04-0.06]	1.4 [1.2-1.5]
Côte d'Ivoire	1.56 [1.54-1.58]	113 [112-114]	269 [263-274]	105 [104-106]	2368 [1038-3698]	1.97 [0.73-3.20]	16.4 [7.2-25.6]
Gambia	1.15 [1.15-1.16]	138 [136-140]	28 [29-30]	134 [132-136]	52 [51-53]	0.02 [0.00-0.05]	0.56 [0.42-0.62]
Ghana	1.39 [1.38-1.40]	131 [129-133]	632 [629-634]	124 [123-125]	2138 [1413-2863]	1.44 [0.76-2.13]	16.6 [10.9-22.3]
Guinea	1.40 [1.39-1.41]	141 [139-143]	76 [66-95]	132 [130-134]	1861 [1659-2063]	1.71 [1.53-1.90]	19.3 [18.2-20.5]
Guinea-Bissau	1.44 [1.43-1.46]	83 [82-84]	20 [19-20]	73 [72-74]	2084 [2040-2128]	1.85 [1.81-1.88]	18.7 [18.6-18.9]
Liberia	1.33 [1.32-1.33]	120 [117-125]	17 [17-18]	111 [110-112]	196 [193-198]	0.17 [0.17-0.18]	2.3 [2.2-2.3]
Mali	1.64 [1.63-1.66]	68 [64-72]	35 [34-37]	59 [55-63]	2254 [2189-2320]	2.00 [1.94-2.06]	1.48 [1.47-1.49]
Mauritania	1.39 [1.36-1.42]	103 [101-104]	119 [116-123]	97 [95-99]	331 [243-420]	0.20 [0.05-2.18]	2.3 [2.1-2.5]
Niger	4.45 [4.37-4.52]	20 [12-28]	86 [84-87]	15 [6-24]	19021 [18597-19444]	10.72 [10.49-10.96]	26.2 [20.0-27.9]
Nigeria	1.67 [1.64-1.69]	121 [117-125]	774 [608-824]	112 [108-116]	21800 [6616-36983]	19.50 [11.89-27.11]	141.0 [126.7-249.8]
Senegal	1.38 [1.37-1.39]	147 [146-152]	136 [133-138]	139 [138-140]	989 [55-2033]	0.82 [0.02-1.81]	9.7 [1.8-17.7]
Sierra-Leone	1.58 [1.56-1.60]	83 [78-88]	31 [30-33]	75 [69-81]	700 [673-727]	0.62 [0.59-0.64]	5.0 [4.9-5.2]
Togo	1.16 [1.16-1.17]	220 [218-222]	21 [15-27]	212 [210-214]	110 [100-121]	0.09 [0.08-0.09]	2.2 [2.0-2.4]
West Africa	1.39 [1.38-1.41]	119 [117-121]	1891 [1874-1909]	111 [108-112]	25267 [24239-26294]	22.21 [21.21-23.22]	248.8 [140.8-250.7]

\mathcal{R}_0 : Basic reproduction number; T_{rp} : Peak time of reported cases; n_{rp} : Peak size of reported cases; T_{pp} : time at which the largest daily number of new infectious cases in the population is obtained; n_{pp} : largest daily number of new infectious cases in the population is obtained; I_{max} : Maximum number of active cases; I_{total} : Total number of cases over the course of the epidemic wave.

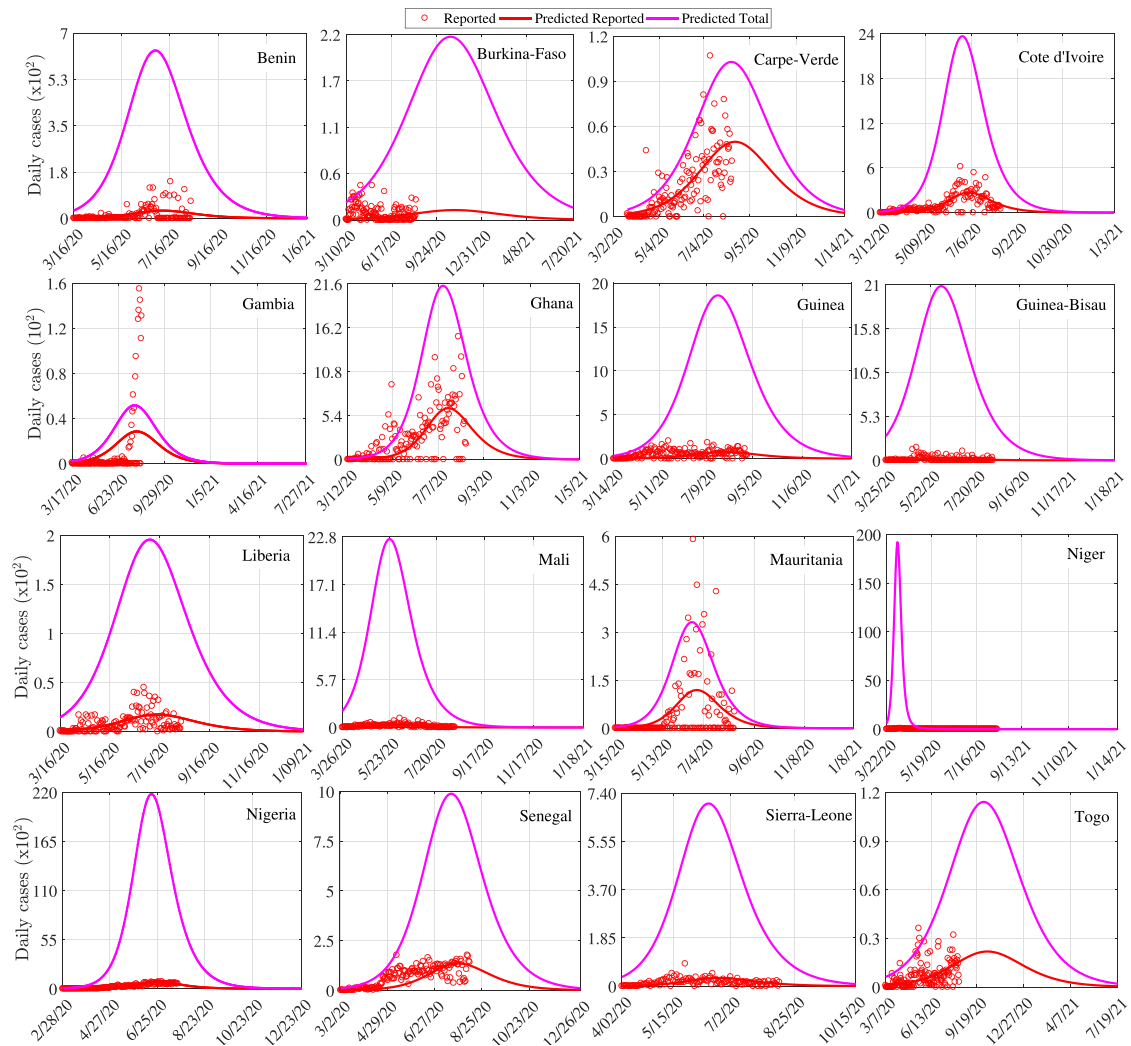


Fig. 1. Evolution trend of the COVID-19 daily cases per west African country for the first wave.

Long-term dynamics of COVID-19 in West Africa

We analyzed the long-term dynamics of COVID-19 in West Africa by first focusing on the true peak of the pandemic. In general, the estimated reported peak time came a week (7–8 days) after the true peak time in all the countries, while their estimated reported peak sizes accounted on average for 21% of the estimated true peak size (Table 2). However, for Cape Verde, Ghana and Mauritania, the estimated peak for the reported cases was much lower than the observed peak, thus revealing a great variability in the reported data with an alternation of days without reported cases and days with a large number of cases. Most countries had already experienced the peak of the epidemic wave. The true peak time was estimated in June for Sierra-Leone (14th), Mauritania (19th), Benin (27th), Côte d'Ivoire (24th) and Ghana (13th), while it was estimated in July for Liberia (4th) and Nigeria (5th), Senegal (18th), Guinea (23th), Cape-Verde (22th) and Gambia (28th). Niger recorded the earliest true peak time (April 8th), while the latest true peak time was on October 26th, 2020 for Burkina-Faso (Fig. 1 and Table 2). The true peak time across the region was 1st July with 25,267 new cases (Table 2 and Fig. 4a–b). The margin error of the estimated true peak time varied from one day to 16 days, with an average value of five days in the region. Half of the countries (8 out of 16) recorded a true peak size of less than 1,000 new cases at the peak time. The highest numbers of new cases at the peak time were estimated at 19,021 and 17,703 for Niger and Nigeria, respectively (Table 2 and Fig. 1). The estimate of the peak size of reported cases was 1,891 daily new cases across the region (Table 2 and Fig. 4a–b).

The final epidemic size accounted for 0.6% of the population of West Africa. This estimate was generally low (< 1% of the population size) for more than half of the countries, though Guinea-Bissau and Cape-Verde recorded the highest final

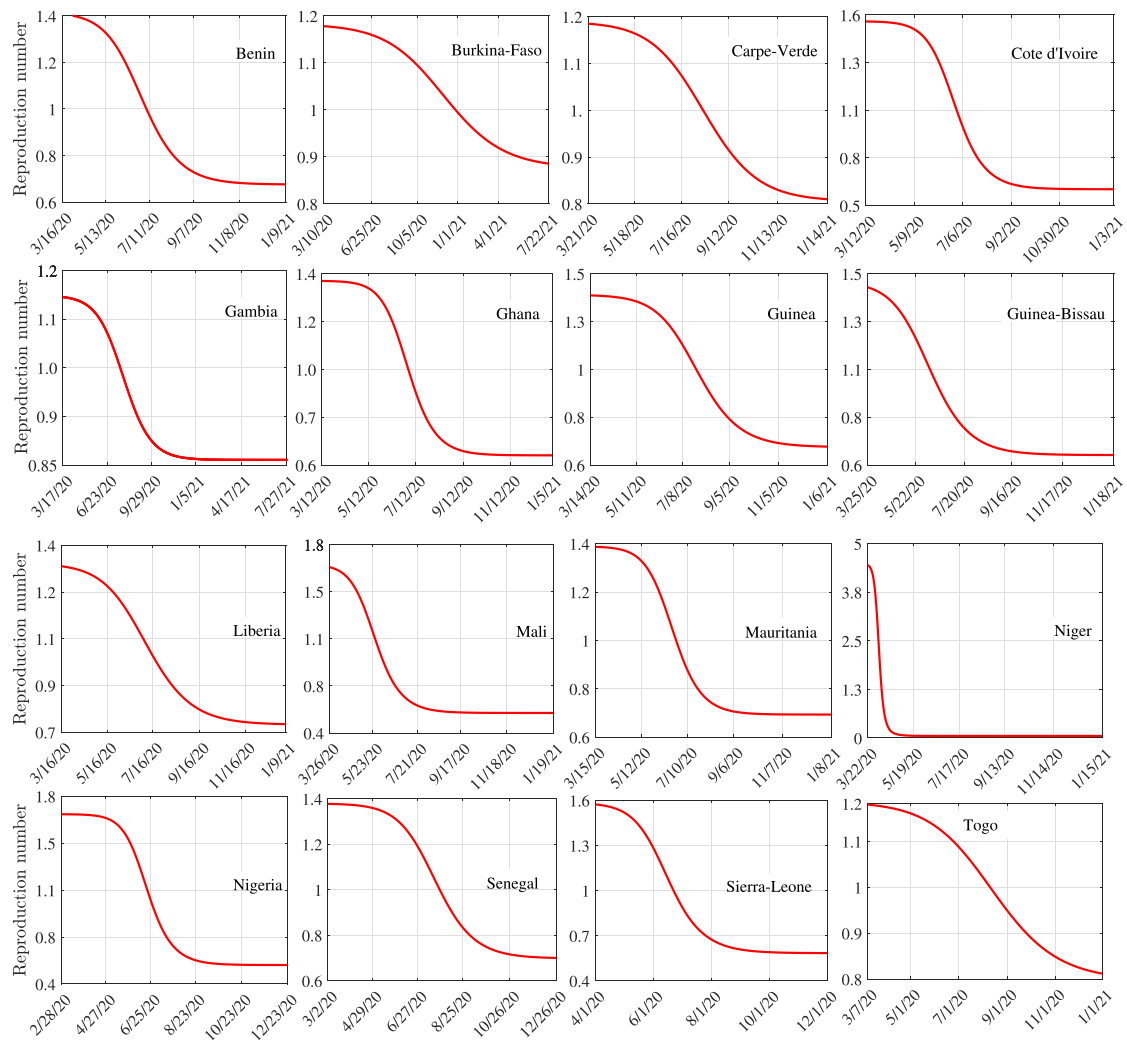


Fig. 2. Running reproduction number per country in West Africa.

epidemic sizes in terms of proportion to their population size ($> 9\%$). The estimates of the maximum number of actual daily active cases at the peak time for most countries were greater than 1,000 cases, though, it was 107,200 and 195,000 for Niger and Nigeria, respectively (Table 2).

The running reproduction number helped to assess the evolution trends of the disease. It decreased over time in all the countries from the beginning of the outbreak (1.2 – 4.5) to a stable point, which varied according to countries (0.50 – 0.82; Fig. 2). As expected, the fraction of susceptible individuals being infected (attack ratio) increased over time from 0% to 40% – 70%, depending on countries. In addition, the maximum of attack ratio exceeded 50% in most of the countries. The evolving trends in the reproduction number and attack ratio were similar to those noted for West Africa as a whole (Fig. 4b–c). Moreover, Fig. 4 reveals that the peak with about 25,300 new cases occurred earlier in July 2020 with an attack ratio of around 0.3.

Discussion

In epidemiology, understanding the dynamics of an epidemic outbreak and predicting its future course is a major research question, which is often studied using modelling techniques [30,31]. Estimation and prediction rely on mathematical and statistical models, which inform public health decision makers and ensure optimal use of resources to reduce the morbidity and mortality associated with epidemics [10,32–34]. For instance, estimation of epidemiological parameters and prediction on the *Influenza* outbreak dynamics in Canada was done using Richard's model [32], while a three-parameter logistic

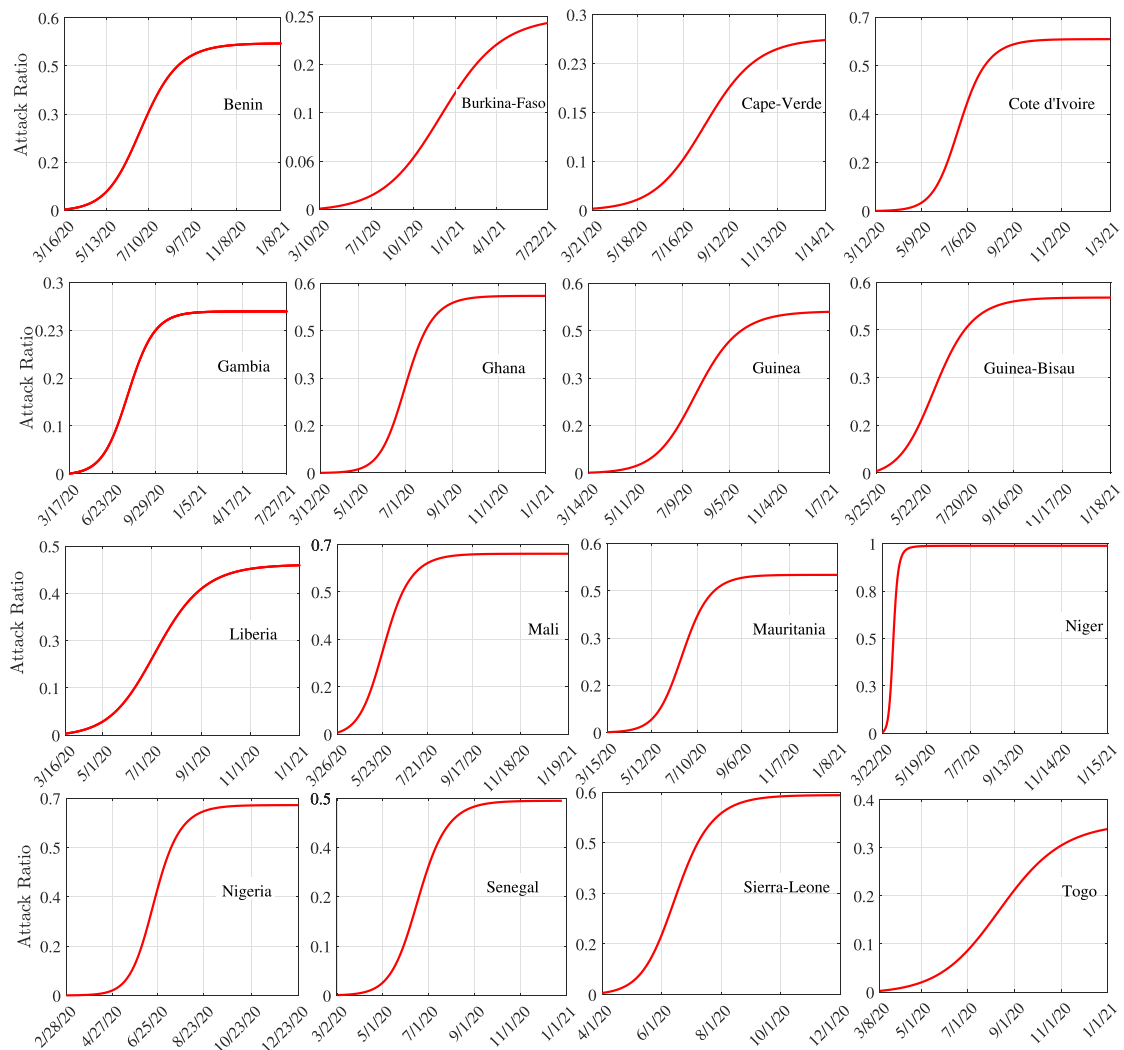


Fig. 3. Evolution trends of the attack ratio per country in West Africa.

growth model was used to study and forecast the final epidemic size in real-time of the *Zika* virus outbreaks in Brazil from 2015 to 2016 [30].

In this study, we used a deterministic SIR-type model to understand COVID-19 dynamics in the West African countries and estimated the overall number of susceptible individuals, which accounted for the 1.2% of the West African population and 1% for most countries, except Guinea-Bissau and Cape Verde, where the susceptible individuals accounted for more than 2%. The concept of susceptibility in this study, considering the model (1) takes into account sensibility and exposure to COVID-19. Thus, the low proportion of susceptible individuals in most countries could be explained by physiological factors, immunity acquired from other diseases or epidemics, or low levels of exposure to the disease (the majority of individuals are far from the epicentre of the pandemic in different countries, with relatively low human movement between remote regions in West Africa as compared to the developed countries). Actually, individuals who are more susceptible or more exposed tend to be infected earlier, depleting the susceptible subpopulation of those who are at higher risk of infection [35]. This selective depletion of susceptible individuals intensifies the deceleration in the incidence. Our findings also revealed a great disparity between countries in terms of the testing rates of COVID-19. Countries such as Guinea and Gambia and to a less extent, Côte d'Ivoire and Nigeria, showed relatively less testing effort to identify many infected individuals. This suggests that there may not be enough tests being carried out to properly monitor the outbreak [25]. In contrast, countries such as Cape-Verde, Benin and Togo, which have recorded less than or equal to 50 positive cases per 1,000 tests, seem to be effectively controlling the pandemic according to the WHO criteria [36]. Compared to relatively wealthier countries such as Australia, South Korea and Uruguay, it takes hundreds of tests to find one case [25].

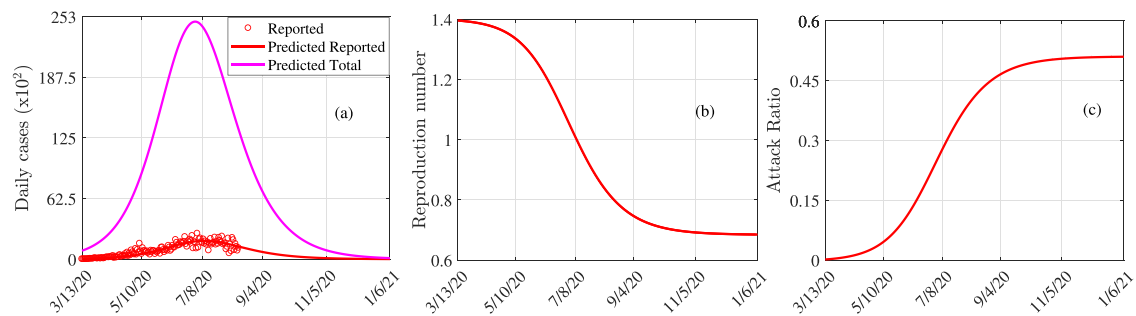


Fig. 4. Trends in COVID-19 dynamics across West Africa. (a) Prediction of the true peak and reported peak date, and size of COVID-19. (b). Evolution trends of the reproduction number. (c) Evolution trends of the attack ratio.

The detection rate considered in model Eq. (1) is a better indicator of the testing effort since it represents the proportion of active cases in the population that are identified daily. Our results revealed a relatively low detection rate of COVID-19 in West Africa with less than 2% in most countries except Gambia, Cape-Verde and Mauritania (> 5%). The last two countries are also the ones with the highest testing rates (Table A1) confirming the link between detection rate and testing effort [37]. The fact that Gambia had a relatively low testing effort and a high detection rate suggests that either an efficiency in the contact tracing and testing efforts directed towards those really exposed, or poor quality of parameter estimation. Indeed, especially for Gambia, the peak size of the reported cases was underestimated by the model compared to the observed data. This may be explained by an unusually long period of very low detection of the disease in the country (March 18 - July 13, 2020). Other factors that may explain significant differences between some estimates and observed data, including data quality are discussed elsewhere [21]. For example, data from Benin showed, from June 30, long periods (4-7 days) without detected cases, often alternating with a large number of detected cases (more than 80) within a single day. This may indicate a possible problem in the daily reporting of data or in the planning of PCR tests and has led to a significant underestimation of the peak of reported cases (Table 2). This was the case in Niger, where very low notification of COVID-19 cases (detection rate of around 0.1%; Table 1) led to a low number of observations and poor quality data, ultimately resulting in a somewhat poor estimation of model parameters.

The fairly low detection rates in most West African countries demonstrate low testing effort and may be explained by a number of factors, including the availability of testing kits and qualified healthcare workers as well as the low ability to control the disease due to their low GDP. For instance, the average detection rate of COVID-19 in the world in April 2020 was estimated at 6% [38]. It is also useful to note that the estimated average detection rate hides a great variability in the testing effort over time. Indeed, it is generally accepted that the testing rate is relatively low at the very beginning of an epidemic outbreak, but can increase rapidly over time when better response mechanisms are put in place [39].

The dynamics of COVID-19 in West Africa show a reproduction number greater than one in all countries (from 1.2 in Burkina-Faso to 4.4 in Niger), while it was 1.4 for the whole region. This value is relatively low compared to 1.6, estimated for the same region in June in a recent study using a modified SEIR model [11]. Hence, this reveals either a declining trend in the pandemic over time or the result of using a different modeling approach to estimate the reproduction number. COVID-19 appears more serious than the Ebola outbreak in Africa given the reproduction number. Indeed, the reproduction number was estimated at 1.1, 1.2 and 1.2 for Guinea, Liberia and Sierra-Leone, respectively, against 1.4, 1.3 and 1.6 for the same countries as far as COVID-19 is concerned [40]. These comparisons indicate that COVID-19 is on average 1.29 times more reproducible than Ebola in these countries.

The trend in the running reproduction number reveals a rapid decline in all the countries except Burkina-Faso and reveals some efficiency of the control measures put in place and being implemented in the different countries. Most countries had already experienced a peak in new COVID-19 cases in June and July 2020. In general, the reported peak was very low compared with the true peak. Moreover, the true peak is relatively low compared with other regions in the world, probably indicating either good preparedness and response to COVID-19 [41], or resilience of Africans to COVID-19 [42], which could be attributed to acquired immunity from past epidemics or even weather conditions limiting the spread of the pandemic in Africa [43].

Outputs from this study are linked to Sustainable Development Goal 3 (Target 3.3 - End epidemics and other communicable diseases) of the United Nations. Similar studies have shown that different approaches have been investigated to understand and predict the dynamics of the pandemic. Indeed, different models, for instance, the Bats-Hosts-Reservoir-People transmission network, model using numerical estimation methods such as VIM were applied to estimate parameters, especially for the unreported cases [44-46]. These investigations are in support of our study findings which show that estimates vary according to time. In addition, a hybrid modeling technique combining compartmental and growth models was also applied to the same data used in this study and yielded robust and more accurate estimations [47]. However, predicting the course of the pandemic based on deterministic or growth models depends on the reliability of the data collected.

Conclusion

Our study shows that the novel COVID-19 pandemic, although highly contagious has not seriously impacted West Africa in terms of prevalence, compared to other parts of the world, particularly Europe and the USA. Actually, the total number of susceptible individuals and final epidemic size account for 1.2% and 0.6% of the total population size of West Africa, respectively. But, the relatively low reported cases are related to very low testing efforts in West African countries. The study also indicates a relatively low detection rate, and for most countries in the region, the dates of the true peak of infection have passed (June-July 2020). In addition, we found out that the minimum value of the basic reproduction number was observed in Burkina-Faso and in Gambia (1.15) while the maximum value was found in Niger (4.45). The maximum attack ratio exceeded 50% in most of the countries and the peak with about 25,300 new cases was predicted earlier in July 2020 with an attack ratio of around 0.3. Nevertheless, the pandemic is still ongoing in the region and it is important that the non-pharmaceutical measures currently in place should continue over time to help reduce its spread dynamics, pending adequate effective treatment or vaccine.

Authors' contributions

RGK conceived the study, designed the methodology, reviewed the simulation algorithm and supervised the work. SHH collected the data, and along with HBT performed numerical simulations and wrote most sections of the manuscript. All authors reviewed the drafts and gave their final approval for publication.

Declaration of Competing Interest

We wish to confirm that there are no known conflicts of interest associated with this publication and there has been no significant financial support for this work that could have influenced its outcome.

Acknowledgments

RGK acknowledges the support from the Humboldt research Hub SEMCA funded by the German Federal Foreign Office with the support of the Alexander von Humboldt Foundation (AvH).

Appendix A. Demographic patterns and testing efforts of the 16 West African countries

Table A1
Demographic patterns and testing efforts of the 16 West African countries.

Countries	Population size	Density	First case	Tests/1M Pop	Cases/1000 tests
Benin	12,123,200	108	03/16/2020	9,711	18
Burkina-Faso	20,946,992	76	03/10/2020	-	-
Cape-verde	556,498	138	03/21/2020	137,485	50
Côte d'Ivoire	26,428,999	83	03/12/2020	4,779	142
Gambia	2,421,823	239	03/17/2020	5,502	222
Ghana	31,072,945	137	03/12/2020	14,183	100
Guinea	13,160,021	53	03/14/2020	1,860	382
Guinea-Bissau	1,971,640	70	03/25/2020	-	-
Liberia	5,066,990	53	03/16/2020	-	-
Mali	20,294,900	17	03/26/2020	1,852	74
Mauritania	4,659,052	5	03/15/2020	14,980	100
Niger	24,269,389	19	03/22/2020	372	130
Nigeria	206,522,290	226	02/28/2020	1,943	134
Senegal	16,776,618	87	03/02/2020	8,632	93
Sierra-Leone	7,989,949	111	04/01/2020	-	-
Togo	8,293,924	152	03/07/2020	7,784	22
West Africa	402,555,230	66	02/28/2020	-	-

Date: 08/31/2020; Source: [26] and [25]; Tests/1M Pop: number of tests per 1 million individuals;
Cases/1000 tests: number of positive cases per 1000 tests; - : no data.

References

- [1] S. Djilali, B. Ghanbari, Coronavirus pandemic: A predictive analysis of the peak outbreak epidemic in South Africa, Turkey, and Brazil, *Chaos Soliton Fract* (2020) 138.
- [2] W.C. Roda, M.B. Varughese, D. Han, M.Y. Li, Why is it difficult to accurately predict the COVID-19 epidemic? *Infect. Dis. Model* 5 (2020) 271–281.
- [3] WHO, Coronavirus disease (COVID-19): Situation Report – 208, 2020, <https://www.who.int/emergencies/diseases/novel-coronavirus-2019/situation-reports>. Accessed: 2020–08–15.
- [4] M. Maleki, M.R. Mahmoudi, D. Wraith, K.H. Pho, Time series modelling to forecast the confirmed and recovered cases of COVID-19, *Travel Med Infect Dis* (2020) 101742.
- [5] M. Sperrin, S.W. Grant, N. Peek, Prediction models for diagnosis and prognosis in Covid-19, *BMJ* (2020) 369, M1328.
- [6] WHO, Global health observatory data, 2020, https://apps.who.int/gho/data/node.main.HWFGRP_0020?lang=en (Accessed 10 April 2020).
- [7] M. Martinez-Alvarez, A. Jarde, E. Usuf, H. Brotherton, M. Bittaye, A.L. Samateh, M. Antonio, J. Vives-Tomas, U. D'Alessandro, A. Roca, COVID-19 pandemic in west Africa, *Lancet Glob. Health* 18 (5) (2020), E631–e632.
- [8] L. Wynants, B. Van Calster, G.S. Collins, R.D. Riley, G. Heinze, E. Schuit, M.M.J. Bonten, D.L. Dahly, J.A.A. Darden, T.P. Debray, V.M.T. de Jong, M. De Vos, P. Dhiman, M.C. Haller, M.O. Harhay, L. Henckaerts, P. Heus, N. Kreuzberger, A. Lohmann, K. Luijken, J. Ma, G.P. Martin, C.L.A. Navarro, J.B. Reitsma, J.C. Sergeant, C. Shi, N. Skoetz, L.J.M. Smits, K.I.E. Snell, M. Sperrin, R. Spijker, E.W. Steyerberg, T. Takada, I. Tzoulaki, S.M.J. van Kuijk, F.S. van Royen, J.Y. Verbakel, C. Wllisch, J. Wilkinson, R. Wolff, L. Hooft, K.G. Moons, M. van Smeden, Prediction models for diagnosis and prognosis of covid-19 infection: systematic review and critical appraisal, *BMJ* (2020) 369, M1328.
- [9] X. Zhang, R. Ma, L. Wang, Predicting turning point, duration and attack rate of COVID-19 outbreaks in major Western countries, *Chaos Soliton Fract* (2020) 109829.
- [10] L. Wang, J. Li, S. Guo, N. Xie, L. Yao, Y. Cao, S.W. Day, S.C. Howard, J.C. Graff, T. Gu, J. Ji, W. Gu, D. Sun, Real-time estimation and prediction of mortality caused by COVID-19 with patient information based algorithm, *Sci. Total Environ.* (2020) 138394.
- [11] B.H. Taboe, V.K. Salako, C.N. Ngonghala, J. Tison, R. Glèlè Kakai, Predicting COVID-19 spread in the face of control measures in West Africa, *Math Biosci* 328 (2020) 108431.
- [12] K. Mizumoto, K. Kagag, G. Chowell, Early epidemiological assessment of the transmission potential and virulence of coronavirus disease 2019 (COVID-19) in wuhan city: China, january-february, 2020, *BMC Med.* 18 (1) (2020) 1–9, doi:10.1186/s12916-020-01691-x.
- [13] J. Ma, Estimating epidemic exponential growth rate and basic reproduction number, *Infect. Dis. Model* 5 (2020) 129–141.
- [14] S. Tuli, S. Tuli, R. Verna, R. Tuli, Modelling for prediction of the spread and severity of COVID-19 and its association with socioeconomic factors and virus types, *medRxiv* (2020), doi:10.1101/2020.06.18.20134874.
- [15] A.J. Kucharski, T.W. Russell, C. Diamond, Y. Liu, J. Edmunds, S. Funk, R.M. Eggo, F. Sun, M. Jit, J.D. Munday, Early dynamics of transmission and control of COVID-19: a mathematical modelling study, *Lancet Infect Dis.* 20 (2020) 553–558.
- [16] C. Iwendi, A.K. Bashir, A. Peshkar, R. Sujatha, J.M. Chatterjee, S. Pasupuleti, R. Mishra, S. Pillai, O. Jo, COVID-19 Patient Health Prediction Using Boosted Random Forest algorithm, *Front. Public Health* 8 (2020) 357.
- [17] A. Onovo, A. Atobatele, A. Kalaiwo, C. Obanubi, E. James, P. Gado, G. Odezugo, D. Ogundehin, D. Magaji, M. Russell, Using supervised machine learning and empirical bayesian kriging to reveal correlates and patterns of COVID-19 disease outbreak in sub-saharan africa: Exploratory data analysis, Available at SSRN (2020) 3580721.
- [18] C.F. Tovissodé, B.E. Lokonon, R. Glèlè Kakai, On the use of growth models for forecasting epidemic outbreaks with application to COVID-19 data, *medRxiv* (2020), doi:10.1101/2020.08.16.20176057.
- [19] M.G. Pedersen, M. Meneghini, Quantifying undetected COVID-19 cases and effects of containment measures in Italy, *ResearchGate Preprint* (online 21 March 2020) (2020), doi:10.13140/RG.2.2.11753.85600.
- [20] N.G.C. Bizet, D.K.M. Peña, Time-dependent and time-independent SIR models applied to the COVID-19 outbreak in Argentina, Brazil, Colombia, Mexico and South Africa, *arXiv preprint arXiv:2006.12479* (2020).
- [21] J. Gnanvi, V.K. Salako, B. Kotanmi, R. Glèlè Kakai, On the reliability of predictions on covid-19 dynamics: a systematic and critical review of modelling techniques, *Infectious Dis. Modell.* 6 (2021) 258–272, doi:10.1016/j.idm.2020.12.008. ISSN 2468-0427
- [22] R.M. Anderson, Discussion: the Kermack-McKendrick epidemic threshold theorem, *B Math. Biol.* 53 (1) (1991) 1–32.
- [23] P. Magal, G. Webb, The parameter identification problem for SIR epidemic models: identifying unreported cases, *J. Math. Biol.* 77 (6–7) (2018) 1629–1648.
- [24] G. Chowell, Fitting dynamic models to epidemic outbreaks with quantified uncertainty: A primer for parameter uncertainty, identifiability, and forecasts, *Infect Dis Model.* 2 (3) (2020) 379–398.
- [25] M. Roser, H. Ritchie, E. Ortiz-Ospina, J. Hasell, Coronavirus Pandemic (COVID-19), Our World in Data (Accessed on August 20, 2020) (2020). <https://ourworldindata.org/coronavirus>.
- [26] Worldometer, African countries by population, 2020, <https://www.worldometers.info/population/countries-in-africa-by-population/> (Accessed on August 14, 2020).
- [27] R.J. Hyndman, A.B. Koehler, Another look at measures of forecast accuracy, *Intern. J. Forecasting* 22 (4) (2006) 679–688.
- [28] MATLAB, Version 9.0.0 (R2016a), Computer Software, The MathWorks Inc., Natick, MA-USA, 2016.
- [29] H.H. Weiss, The SIR model and the foundations of public health, *Materials mathematics* (2013) 01–17.
- [30] S. Zhao, S.S. Musa, H. Fu, D. He, J. Qin, Simple framework for real-time forecast in a data-limited situation: the Zika virus (ZIKV) outbreaks in Brazil from 2015 to 2016 as an example, *Parasite Vector.* 10 (1) (2016) 366–378.
- [31] D. He, D. Gao, Y. Lou, S. Zhao, S. Ruan, A comparison study of Zika virus outbreaks in French Polynesia, Colombia and the State of Bahia in Brazil, *Sci Rep.* 7 (2017) 273.
- [32] Y.H. Hsieh, Richards model: a simple procedure for real-time prediction of outbreak severity in *Modeling and dynamics of infectious diseases*, *World Scientific* (2009) 216–236.
- [33] J. Wangping, H. Ke, S. Yang, C. Wenzhe, W. Shengshu, Y. Shanshan, W. Jianwei, K. Fuyin, T. Penggang, L. Jing, L. Miao, H. Yao, Extended SIR prediction of the epidemics trend of COVID-19 in Italy and compared with Hunan, China, *Front. Med-Lausanne* 7 (2020) 169.
- [34] S. He, S. Tang, L. Rong, A discrete stochastic model of the COVID-19 outbreak: Forecast and control, *Math Biosci Eng.* 17 (2020) 2792–2804.
- [35] M.G. Gabriela, M.C. Rodrigo, G.K. Jessica, E.L. Kate, C. Souto-Maior, J. Carneiro, G. Gonçalves, C. Penha-Gonçalves, U.F. Marcelo, R. Aguas, Individual variation in susceptibility or exposure to SARS-CoV-2 lowers the herd immunity threshold, *MedRxiv* (2020), doi:10.1101/2020.04.27.20081893.
- [36] WHO, Public health criteria to adjust public health and social measures in the context of COVID-19, annex to Considerations in adjusting public health and social measures in the context of COVID-19, 2020,
- [37] S. Phipps, R.Q. Grafton, T. Kompas, Estimating the true (population) infection rate for COVID-19: A Backcasting Approach with Monte Carlo Methods, *medRxiv preprint* (2020), doi:10.1101/2020.05.12.20098889.
- [38] C. Bommer, S. Vollmer, Average detection rate of SARS-CoV-2 infections is estimated around six percent, *Lancet Infect Dis.* (2020).
- [39] R. Omori, K. Mizumoto, G. Chowell, Changes in testing rates could mask the novel coronavirus disease (COVID-19) growth rate, *Int J Infect Dis.* 94 (2020) 116–118.
- [40] X.S. Wang, L. Zhong, Ebola outbreak in West Africa: real-time estimation and multiple-wave prediction, *arXiv preprint arXiv:1503.06908* (2015).
- [41] I.A. Ossenii, COVID-19 pandemic in sub-saharan africa: preparedness, response, and hidden potentials, *Tropical Medicine and Health* 48 (2020) 48.
- [42] C. Ihekweazu, E. Agogo, Africa's response to COVID-19, *BMC Medicine* 18 (2020) 151.
- [43] S.A. Meo, A.A. Abukhalaf, A.A. Alomar, T.W. Aljudi, H.M. Bajri, W. Sami, J. Akram, S.J. Akram, W. Hajjar, Impact of weather conditions on incidence and mortality of COVID-19 pandemic in africa, *European Review for Medical and Pharmacological Sciences* 24 (2020) 9753–9759.

- [44] W. Gao, P. Veerasha, D.G. Prakasha, H.M. Baskonus, Novel Dynamic Structures of 2019-nCoV with Nonlocal Operator via Powerful Computational Technique, *Biology* 9 (5) (2020) 107.
- [45] W. Gao, P. Veerasha, H.M. Baskonus, D.G. Prakasha, P. Kumar, A new study of unreported cases of 2019-nCoV epidemic outbreaks, *Chaos Solitons Fractals* 138 (109929) (2020) 1–6.
- [46] W. Gao, H.M. Baskonus, L. Shi, New investigation of bats-hosts-reservoir-people coronavirus model and application to 2019-nCoV system, *Adv Differ Equ* 2020 (391) (2020) 1–11.
- [47] C.F. Tovissode, T.J. Doumate, R. Glèlè Kakaï, A Hybrid Modeling Technique of Epidemic Outbreaks with Application to COVID-19 Dynamics in West Africa, *Biology* 10 (5) (2021) 365.